

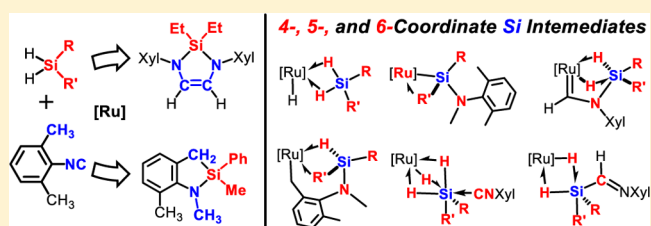
Significant Cooperativity Between Ruthenium and Silicon in Catalytic Transformations of an Isocyanide

Mark C. Lipke,[†] Allegra L. Liberman-Martin,[‡] and T. Don Tilley*[‡]

Department of Chemistry, University of California, Berkeley, California 94720, United States

S Supporting Information

ABSTRACT: Complexes $[\text{PhBP}_3]\text{RuH}(\eta^3\text{-H}_2\text{SiRR}')$ ($\text{RR}' = \text{Me, Ph, 1a}$; $\text{RR}' = \text{Ph}_2, \text{1b}$; $\text{RR}' = \text{Et}_2, \text{1c}$) react with XylNC to form carbene complexes $[\text{PhBP}_3]\text{Ru}(\text{H})=[\text{C}(\text{H})(\text{N}(\text{Xyl})(\eta^2\text{-H-SiRR}'))]$ (**2a–c**; previously reported for **2a,b**). Reactions of **1a–c** with XylNC were further investigated to assess how metal complexes with multiple M–H–Si bonds can mediate transformations of unsaturated substrates. Complex **2a** eliminates an *N*-methylsilacycloindoline product (**3a**) that results from hydrosilylation, hydrogenation, and benzylic C–H activation of XylNC . Turnover was achieved in a pseudocatalytic manner by careful control of the reaction conditions. Complex **1c** mediates a catalytic isocyanide reductive coupling to furnish an alkene product (**4**) in a transformation that has precedent only in stoichiometric processes. The formations of **3a** and **4** were investigated with deuterium labeling experiments, KIE and other kinetic studies, and by examining the reactivity of XylNC with an $\eta^3\text{-H}_2\text{SiMeMes}$ complex (**1d**) to form a C–H activated complex (**6**). Complex **6** serves as a model for an intermediate in the formation of **3a**, and NMR investigations at -30°C reveal that **6** forms via a carbene complex (**1d**) that isomerizes to aminomethyl complex **7d**. These investigations reveal that the formations of **3a** and **4** involve multiple 4-, 5-, and 6-coordinate silicon species with 0, 1, 2, or 3 Ru–H–Si bonds. These mechanisms demonstrate exceptionally intricate roles for silicon in transition-metal-catalyzed reactions with a silane reagent.



INTRODUCTION

There is growing interest in cooperation¹ between transition metals and semimetal species (e.g., boron,² silicon,³ germanium,⁴ etc.) in mediating chemical reactivity. For example, borane and boryl groups participate in the activation of E–H ($\text{E} = \text{H, Si, C}$) bonds at transition metal centers (e.g., Ni ,^{2d,e} Co ,^{2f} Fe ,^{2g} Pt ,^{2h,i} Ir ,^{2b,c} Scheme 1A), and these processes have been incorporated into hydrogenation,^{2d} hydrosilylation,^{2e} and C–H borylation reactions.^{2b,c} During transformations in metal–boron systems, the formation of a M–H–B 3-center 2-electron bond allows the boron center to assist the metal in activating an E–H bond of the substrate.² More complex modes of cooperation are possible, considering the wide range of bonding motifs that exist for semimetal–transition metal complexes.^{4–8} It is important to investigate these possibilities since more intricate modes of cooperation could provide new approaches to challenging transformations. For example, cooperation between rhenium, tethered borane groups, and a bulky base has enabled the stoichiometric reductive coupling of CO using unusually mild reducing conditions (e.g., 1 atm of H_2 , Scheme 1B)⁹ relative to those previously employed (e.g., high pressure H_2 , U(III) , Na^0 , B^0 , Cr(I) , Mg(I)) for reductive coupling of CO or related molecules (e.g., isocyanides).^{2g,10,11}

Silicon also shows considerable promise for cooperative reactivity with transition metals,³ and this possibility might be facilitated by a wide variety of structures that can form between metals and silicon. This laboratory has investigated metal–metalloid cooperation in ruthenium complexes that feature

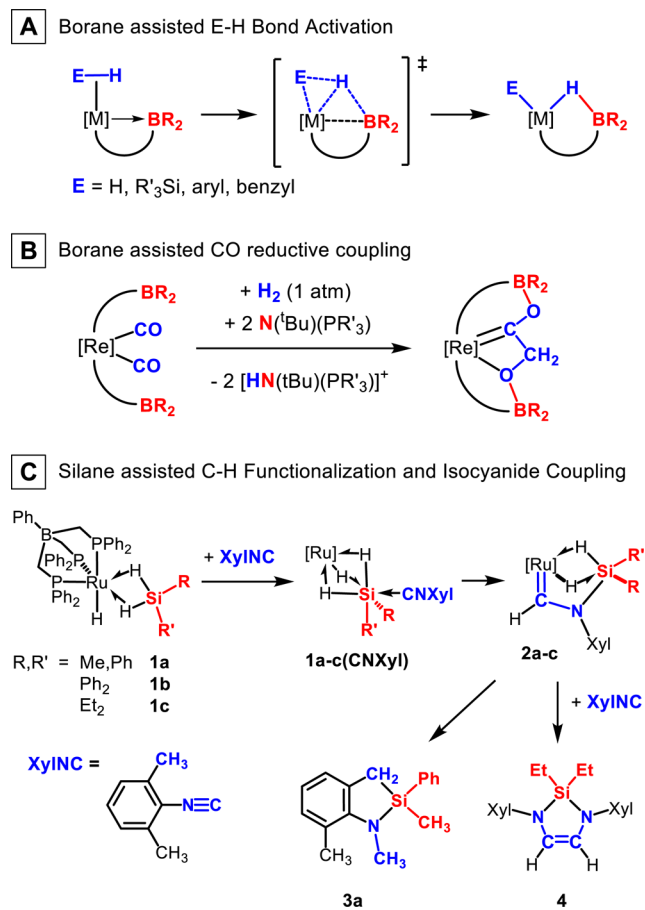
multiple Ru–H–Si 3-center 2-electron bonds.¹² These interactions stabilize hypercoordinate silicon species (e.g., $[\text{ArSiH}_4]^-$ and $[\text{SiH}_6]^{2-}$ anions)^{12b} in the coordination sphere of ruthenium, and mediate low-energy interconversions between structures with different coordination geometries at silicon. Such processes are potentially useful in catalytic transformations, as indicated in the recent discovery that electrophilic Si–H σ -complexes ($[\text{PhBP}_3]\text{RuH}(\eta^3\text{-H}_2\text{SiRR}')$, $\text{RR}' = \text{PhMe, 1a}$; $\text{Ph}_2, \text{1b}$, Scheme 1C) activate an isocyanide substrate (XylNC , $\text{Xyl} = 2,6\text{-dimethylphenyl}$) via a 6-coordinate silicon intermediate.¹³ This process results in formation of carbene complexes **2a,b** that possess a 5-coordinate silicon center.

As described below, this isocyanide transformation can be combined with a subsequent C–H activation to result in elimination of the silacycloindoline product **3a** from carbene complex **2a** (Scheme 1C). Pseudocatalytic turnover for conversion of a silane and isocyanide to **3a** was achieved with careful control of reaction conditions. Interestingly, a related carbene complex **2c** (derived from the $\eta^3\text{-H}_2\text{SiEt}_2$ complex **1c**) is a key intermediate in the reductive coupling of two isocyanides to form a C=C bond in the cyclic product **4** (Scheme 1C). Notably, catalytic turnover was observed for this reaction, whereas related examples of isocyanide reductive coupling have been limited to stoichiometric transformations.¹¹

Received: June 4, 2016

Published: July 6, 2016

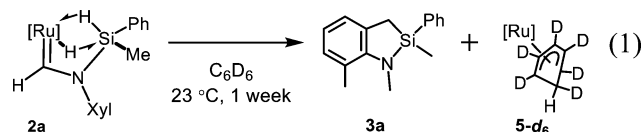
Scheme 1. Examples of Cooperative Reactivity Involving Transition Metals and Metalloid Species



The mechanism of the formation of **3a** was examined in detail to reveal that multiple four-, five-, and six-coordinate silicon intermediates are important in this transformation. Similar structures appear to be relevant for formation of the C=C coupling product **4**. In these mechanisms, the extraordinary coordinative flexibility displayed by silicon is important for binding and activating the isocyanide, stabilizing or destabilizing different coordination environments at ruthenium, and protecting the metal center from deactivation. These results illustrate particularly intricate roles for a main group species in transition metal-catalyzed reactions, and therefore this system provides new insight into the role that silanes or other semimetals species might play in catalytic transformations.

RESULTS AND DISCUSSION

Formation of 3a by C-H Functionalization. The carbene complex **2a** slowly converts (ca. 1 week at 23 °C, monitored by ^1H NMR spectroscopy) to a new organosilicon product (**3a**, eq 1) and the previously reported η^5 -cyclo-



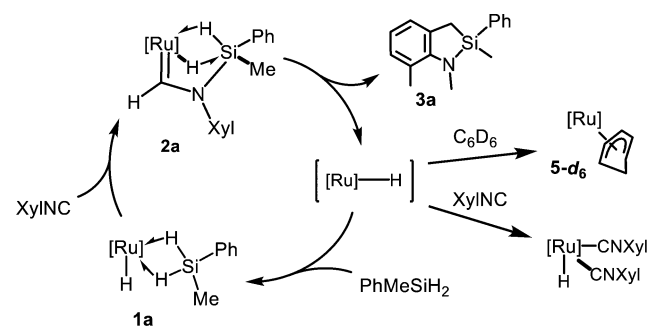
hexadienyl complex $[\text{PhBP}_3]\text{Ru}(\eta^5\text{-C}_6\text{D}_6\text{H})$ (**5-d₆**).¹⁴ The organosilicon product was isolated from the ruthenium product

by distillation, and this allowed full characterization of **3a** as a silacycloindoline derivative. The ^1H NMR spectrum of **3a** in benzene-*d*₆ exhibits three singlet resonances for the three methyl groups (^1H δ 2.82 ppm, NCH_3 ; 2.40, ArCH_3 ; 0.34, SiCH_3), and two doublets for the diastereotopic methylene hydrogens (^1H δ 2.12, 1.97 ppm, $^2J_{\text{HH}} = 18.2$ Hz). The assignments of the ^1H NMR spectrum are supported by a ^{29}Si -filtered ^1H NMR experiment that indicates two- and three-bond coupling for the appropriate ^1H NMR resonances ($^2J_{\text{SiH}} = 7.5$ Hz (Si-CH_3), 7.2 Hz (SiCH_2Ar); $^3J_{\text{SiH}} = 2.8$ Hz (Si-N-CH_3)).¹⁵

Interestingly, **3a** is the product of a multistep transformation involving the hydrosilylation and hydrogenation of the isocyanide group, and functionalization of a benzylic C-H bond with silicon. The functionalization of C-H bonds with silicon has recently been an area of intense interest and can be promoted by the addition of hydrogen acceptors or by installation of silicon into a substrate via hydrosilylation.¹⁶ However, the formation of **3a** appears to be a unique example in which the hydrosilylation step, the hydrogen accepting step, and the C-H functionalization are all combined into a single mechanistic pathway. Further development of these types of reactions could provide atom economical C-H functionalizations, since the isocyanide group plays multiple roles as a directing group and hydrogen acceptor, while also undergoing transformation into a common functional group (methylamino). Thus, attempts were made to determine whether or not the formation of **3a** could be accomplished in a catalytic manner.

It seemed possible that in the presence of excess PhMeSiH_2 , the conversion of **2a** to **3a** might be accomplished with regeneration of the silane complex **1a** from a Ru-H intermediate that otherwise goes on to form unreactive **5-d₆** (Scheme 2).¹⁴ The regeneration of **1a** would allow for the

Scheme 2. Potential Catalytic Cycle for 3a

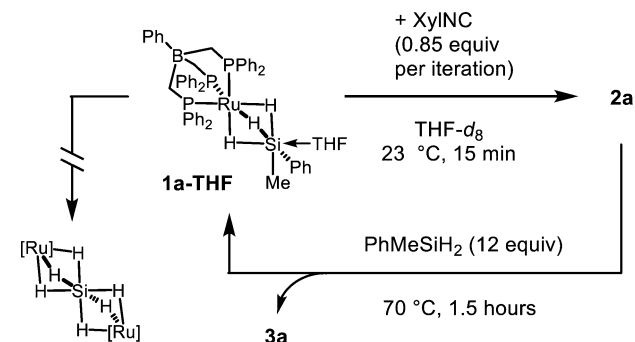


formation of **3a** in a catalytic process, but initial efforts to obtain catalytic turnover were unsuccessful. Treatment of **2a** (at room temperature or 60 °C in benzene-*d*₆) with excess PhMeSiH_2 (20 equiv) and XylINC (20 equiv) resulted in formation of only 1 equiv of **3a** relative to **2a**, and the cyclohexadienyl complex **5-d₆** was the only $[\text{PhBP}_3]\text{Ru}$ product detected by ^1H NMR spectroscopy. To avoid the formation of **5-d₆**, the same reaction with THF-d_8 as the solvent was examined, but these conditions also failed to yield **3a** in a catalytic manner. However, under these conditions a doublet of triplets Ru-H ^1H NMR resonance (-6.68 ppm) was observed and is consistent with formation of a $[\text{PhBP}_3]\text{RuH}(\text{CNXyl})_2$ complex (Scheme 2), on the basis of comparison to a similar ^1H NMR resonance for $[\text{PhBP}_3]\text{RuH}(\text{CO})_2$.¹³ Note that the

coordination of XylNC to ruthenium has previously been shown to prevent formation of carbene complex **2a**, as indicated by the stability of the isocyanide complex $[\text{PhBP}_3]\text{-Ru}(\text{H})(\text{CNXyl})(\eta^2\text{-H-SiHMePh})$.¹³ The catalytic formation of **3a** was also attempted by using a large excess of PhMeSiH_2 , but heating a mixture of **2a** with XylNC (20 equiv) to 60 °C using neat PhMeSiH_2 as the solvent also failed to provide catalytic formation of **3a**. Instead, a mixture of organic/organosilicon compounds was obtained and these products could not be identified.

Turnover for formation of the C–H functionalized product **3a** was ultimately facilitated by careful addition of XylNC to the reaction (Scheme 3). The isocyanide was added in 0.85 equiv

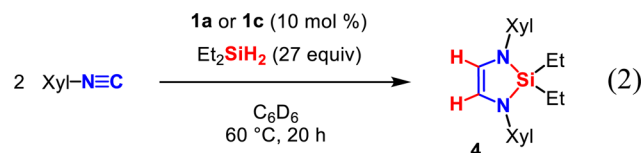
Scheme 3. Pseudocatalytic Formation of **3a**



portions to a solution of the THF adduct of **1a** (**1a-THF**, 1 equiv in $\text{THF-}d_8$) and PhMeSiH_2 (12 equiv). This allows the mixture to be heated (70 °C for 1.5 h) to form **3a** with regeneration of **1a-THF** (Scheme 3) in the absence of excess isocyanide. This process was repeated a total of 5 times to provide **3a** in 70% yield (3 turnovers per ruthenium), at which point only 20% of the active catalyst remained in solution (determined by ^1H NMR spectroscopy). The formation of **3a** in this process relies on stabilization of the silane complex as the THF adduct **1a-THF**, an off-cycle species. The formation of this 6-coordinate silicon species appears to inhibit Si–C cleavage processes that have been observed to result in formation of $\{[\text{PhBP}_3]\text{Ru}\}_2[\mu\text{-}\eta^4,\eta^4\text{-SiH}_6]$ when **1a** is heated in the presence of excess PhMeSiH_2 (Scheme 3).^{12b} The productive mechanistic pathway is enabled by the dissociation of THF to provide **1a**,^{12a} which is responsible for activation of the isocyanide.¹³

Catalytic Reductive Coupling of XylNC by **1c.** The $\eta^3\text{-H}_2\text{SiEt}_2$ complex **1c** also reacted with XylNC to form a carbene complex analogous to **2a,b** (**2c**, Scheme 1C). Complex **2c** formed in nearly quantitative yield (>95% yield by ^1H NMR spectroscopy), and was isolated as an analytically pure white powder (91% isolated yield). Like the SiMePh carbene derivative **2a**, complex **2c** eliminates an organosilane product (**3c**) that appears to be similar to **3a** (by ^1H NMR spectroscopy, see the Supporting Information). This process was slower for **2c** (90% conversion after 4 h at 80 °C in C_6D_6) than for **2a** (90% conversion after 25 min at 80 °C in C_6D_6). The organosilane product **3c** could not be separated from the byproduct **5-d₆** that formed in this stoichiometric reaction, and as a result **3c** was not isolated and fully characterized. However, comparison of the NMR data obtained for **3c** (prepared in situ) to that of pure **3a** supported its identification as a close analogue of **3a** (see the Supporting Information).

Interestingly, while **3c** forms from **2c** in the absence of other reagents, the formation of a different product (a cyclic 1,2-diaminoalkene, **4**, eq 2) was observed (by ^1H NMR



spectroscopy) while investigating possible catalytic conditions for the formation of **3c**. Treatment of a mixture of XylNC and excess Et_2SiH_2 (27 equiv) with **1c** (10 mol %) in benzene- d_6 for 20 h at 60 °C provided **4** in 54% yield (determined by ^1H NMR spectroscopy). Catalysis was also effective when **1c** was generated in situ by adding **1a** to the solution of excess Et_2SiH_2 prior to adding the isocyanide substrate. The formation of **4** results from the hydrosilylation and reductive coupling of two isocyanide groups, and the identity of this product was confirmed by the independent preparation of a sample from glyoxal, XylNH₂, and Et_2SiCl_2 .¹⁷

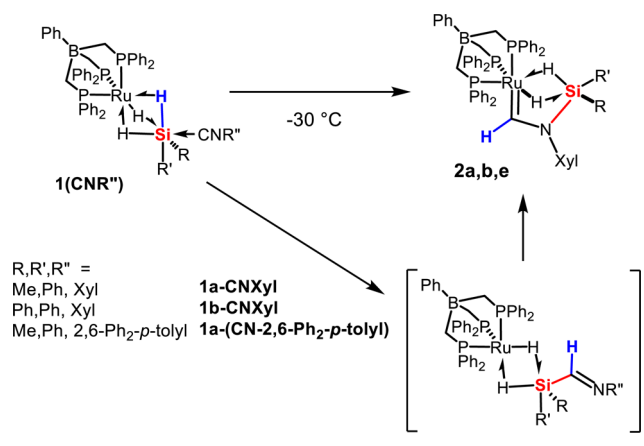
The alkene product **4** is similar to products obtained in previous examples of isocyanide or carbon monoxide reductive coupling reactions that have been studied since the 1970s.¹¹ However, previous examples of isocyanide reductive coupling have been limited to stoichiometric transformations that utilize strong reducing agents (e.g., Zn, Na, Cr(I) dimers, Mg(I) dimers).¹¹ In contrast, the 54% yield of **4** corresponds to 2.7 turnovers of the ruthenium catalyst and utilizes Et_2SiH_2 as a mild reducing agent. These findings are notable since isocyanide reductive coupling reactions can provide insight into reductive couplings that utilize the closely related substrate carbon monoxide. Transformations of the latter type could be important for producing fuels and fine chemicals from this common C_1 -feedstock, but typically require harsh conditions (e.g., high temperatures and pressures) for catalytic processes.¹⁰

Mechanistic Investigations. As described above, the reactions that produce **3a** and **4** are interesting transformations that exhibit several unique features. Thus, it was of interest to better understand the role of nonclassical $\text{Ru}(\text{H})_n\text{-Si}$ ($n = 1\text{--}3$) structures in mediating these unusual transformations. This mechanistic insight could prove useful for development of other tandem hydrosilylation and C–H functionalization reactions that are related to the reaction that forms **3a**. Additionally, insight into the mild catalytic C=C reductive coupling process that forms **4** could enable the development of similar processes using CO as a substrate. Note, however, that this possibility cannot be realized in the present system since CO easily displaces the silane ligand from ruthenium, and $[\text{PhBP}_3]\text{Ru}(\text{CO})_2\text{H}$ is not reactive.¹³

Previously described computational and experimental studies indicate that formation of the intermediates **2a,c** occurs via binding of the isocyanide to the silicon center of the $\eta^3\text{-H}_2\text{SiRR}'$ complexes **1a,c** to form $[\text{PhBP}_3]\text{Ru}(\mu\text{-H})_3[\text{Si}(\text{RR}')\leftarrow\text{CNXyl}]$ (**1a,c-CNXYl**) intermediates (Scheme 1C).¹³ This activates the isocyanide carbon toward attack by the hydride of a Ru-H-Si linkage, to form a Si-C(H)=NXyl species that rapidly isomerizes to the carbene structure (Scheme 4).

It is worth noting that an alternative isocyanide activation pathway might involve equilibration of **1a,c** with electrophilic silylene complexes. It has recently been shown that **1a,c** exist in equilibrium with silylene complexes, but these investigations suggest that it is unlikely that these latter species are involved in

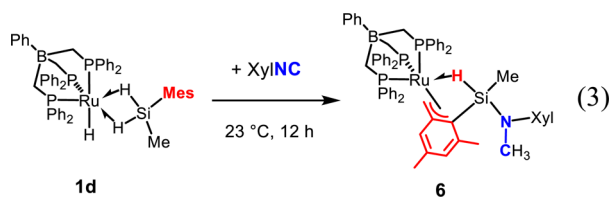
Scheme 4. Mechanism of Formation of 2a–e



activating the isocyanide. The silylene complexes appear to be significantly higher in energy than the silane σ -complexes,¹⁴ and an additional energy barrier for accessing the silylene complexes is created by the binding of XylNC to the silicon center of **1a,c**.¹³ Furthermore, a transient 16 e⁻ silylene complex [PhBP₃]Ru(H)=SiMe₂ was trapped by XylNC to form an adduct with the isocyanide bound to ruthenium, rather than the isocyanide reacting at silicon. Thus, it is unlikely that the high energy silylene intermediates are responsible for the facile formation of **2a,c**, but the aforementioned observations do not definitively rule out the possibility.

The isocyanide activation pathway depicted in Scheme 4 is further supported by kinetic studies of the formations of **2a**, **2b**, and an additional carbene complex **2e** derived from **1a** and the bulky isocyanide (2,6-Ph₂-p-tolyl)NC (Scheme 4). At -30 °C, the rates for conversion of the respective isocyanide adducts to the carbene complexes **2a**, **2b**, and **2e** differ by less than a factor of 3 (see the Supporting Information). The minimal influence of steric effects is consistent with a transition state for the C–H bond forming step in which the SiRR' and NR'' groups have not moved much from their starting geometries in the isocyanide adducts. Such a transition state was previously predicted by DFT calculations for the rate-determining step in the formation of **2a** from **1a**-CNXyl.¹³

Insight into the mechanism of the formation of **3a** from **2a** was obtained by examining the reaction of the η^3 -H₂SiMeMes complex **1d** with XylNC, which nonetheless provided a product distinct from those formed from **1a**–**c** and XylNC. The yellow color of **1d** immediately disappeared upon addition of XylNC (1 equiv in benzene-*d*₆), and the resulting colorless solution developed an intense yellow color within 10 min. The yellow color results from the formation of a new complex (**6**, eq 3),



and this reaction was complete after 12 h (as monitored by ¹H NMR spectroscopy). Complex **6** was isolated as an analytically pure microcrystalline powder after recrystallization from toluene/pentane at -30 °C.

The solid state structure of **6** was determined by single crystal XRD analysis (Figure 1), but the quality of the data is

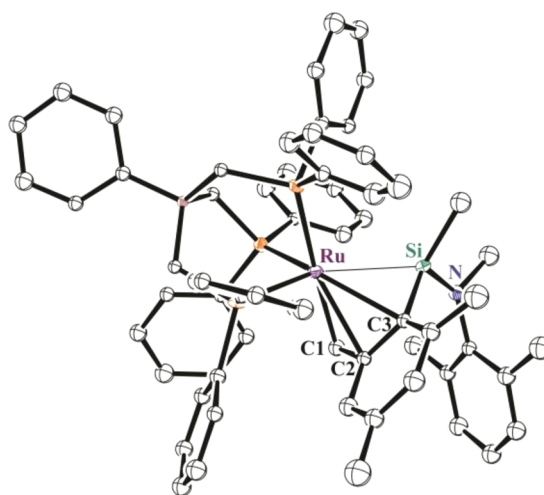


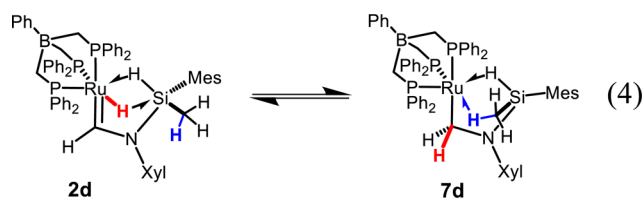
Figure 1. Solid-state structure of **6** determined by single-crystal X-ray diffraction analysis.

relatively low since only small single crystals of **6** could be obtained. As a result of the relatively weak diffraction data, only atoms heavier than carbon could be anisotropically refined. However, all bond angles and distances for common moieties (e.g., the [PhBP₃]Ru fragment and common organic groups) are chemically reasonable,¹⁸ and this structure is consistent with the identity of **6** determined in solution by a variety of NMR experiments (see below). Given this additional information, the structure presented in Figure 1 appears to be a valid representation of the connectivity of **6** despite the poor data available. The structure indicates that **6** is a benzyl complex derived from C–H activation of the Si–Mes group. A fully formed NCH₃ group was also observed. The Ru–Si distance ($d_{\text{Ru–Si}} = 2.683(4)$ Å) in this structure is too long to indicate a strong direct Ru–Si bond. Instead, the Ru–Si distance is consistent with the presence of an agostic Si–H→Ru interaction with a relatively weak H → Ru component. This could not be directly confirmed due to the low quality of the structure, but NMR data clearly support this description (see below).^{7,19}

The structure of **6** was confirmed in solution (benzene-*d*₆) by a variety of NMR experiments. The hydride ligand appears as a doublet in the ¹H NMR spectrum (δ -8.73 ppm, $J_{\text{PH}} = 11$ Hz) integrating as one hydrogen. This hydride resonance exhibits strong J -coupling to silicon ($J_{\text{SiH}} = 108$ Hz from a ²⁹Si-filtered ¹H{³¹P} NMR spectrum), consistent with the presence of a weakly perturbed Si–H bond coordinated to a metal.¹⁹ The ²⁹Si–¹H HMBC NMR spectrum reveals a ²⁹Si resonance (²⁹Si δ -8 ppm) that is coupled to the hydride signal and two other ¹H NMR resonances. The latter resonances each integrate as 3 hydrogens in the ¹H NMR spectrum, and can be assigned to the NMe (¹H δ 2.65 ppm, $^3J_{\text{SiH}} = 3.4$ Hz) and the SiMe (¹H δ 0.99, $^2J_{\text{SiH}} = 7$ Hz) groups.¹⁵ The diastereotopic hydrogens of the RuCH₂Ar group are observed in the ¹H NMR spectrum in benzene-*d*₆ (¹H δ 2.13, 3.41 ppm, 1 H each) and these assignments were supported by 1D and 2D NMR experiments conducted at -10 °C in CD₂Cl₂ (e.g., ¹³C{¹H}, COSY, ¹H–¹³C HSQC, see the Supporting Information). Additionally, both aromatic hydrogens of the activated mesityl group are observed in the ¹H NMR spectrum (¹H δ 4.85, 4.15 ppm) collected at -70 °C. Notably, complex **6** features a fully formed NCH₃ group and a Ru–C bond formed by benzylic C–H

activation. Thus, **6** may serve as a model for intermediate species involved in the formation of the C–H functionalized product **3a** from **2a**.

Information regarding the formation of **6** was obtained by observation of intermediates by NMR spectroscopy at $-40\text{ }^{\circ}\text{C}$ in toluene- d_6 (note that broad resonances were observed in the ^1H NMR spectrum collected at $23\text{ }^{\circ}\text{C}$). A carbene species (**2d**, eq 4) was identified by characteristic ^1H NMR resonances (^1H



δ 10.67 ppm, Ru=CH; -7.02 , -7.42 ppm, RuH) that are similar to those observed for **2a** at this temperature.¹³ An aminomethyl complex (**7d**, eq 4) was also identified in the reaction mixture by a variety of NMR experiments. In particular, the ^1H NMR spectrum ($-40\text{ }^{\circ}\text{C}$) exhibited resonances corresponding to the diastereotopic CH hydrogens of the Ru(CH₂NRR') group (^1H δ 3.72, 2.88 ppm) and to an Si–H→Ru interaction (^1H δ -4.94 ppm, $J_{\text{SiH}} = 104$ Hz). An additional upfield ^1H NMR resonance (δ -1.55 ppm) indicates the presence of an agostic C–H→Ru interaction that is fluxional among three C–H bonds. The identity of **7d** was confirmed by several heteronuclear 2D-NMR experiments described in the Supporting Information. The RuH resonances for **2d** and **7d** exhibit coalescence at $20\text{ }^{\circ}\text{C}$, which indicates that the two species exist in equilibrium (eq 4). The thermodynamic parameters for this equilibrium ($\Delta H_{2\text{d}\rightarrow 7\text{d}} = -3.44$ kcal/mol, $\Delta S_{2\text{d}\rightarrow 7\text{d}} = -12.0$ eu) were determined by a van't Hoff analysis.

The identities of **2d** and **7d** are supported by DFT calculations that provided the structures **2d**-DFT and **7d**-DFT (Figure 2).²⁰ The structure **7d**-DFT (Figure 2b) includes the agostic SiCH₂–H→Ru interaction indicated by the ^1H NMR spectrum of **7d**, and it was not possible to locate an aminomethyl structure without this interaction. The aminomethyl structure (**7d**-DFT) is similar in energy to the carbene structure (**2d**-DFT, Figure 2a, $\Delta G_{2\text{dDFT}\rightarrow 7\text{dDFT}} = +2.3$ kcal/mol), and this is consistent with observation of both **2d** and **7d** in solution. Reversible 1,2-hydride migration processes have been observed for other Fischer carbene complexes and their corresponding amino- or alkoxy-methyl complexes,²¹ but **2d** and **7d** represent the first carbene/methyl complex pair for which both isomers are observed simultaneously. Carbene complexes **2a**–**c** might also exist in equilibrium with their aminomethyl isomers (**7a**–**c**), and this isomerization process may be important to the formation of the organosilicon products **3a** and **4**. However, unlike for the SiMeMes derivatives **2d/7d**, the carbene complexes **2a**–**c** must be considerably more stable than the aminomethyl isomers **7a**–**c** since the latter are not observed in solution by ^1H NMR spectroscopy. This possibility is supported by DFT calculations that located an optimized aminomethyl structure **7a**-DFT that is significantly higher in energy than the corresponding carbene structure **2a**-DFT ($\Delta G_{2\text{aDFT}\rightarrow 7\text{aDFT}} = +10.0$ kcal/mol).

The structures of the SiMePh derivatives **2a**-DFT and **7a**-DFT are similar to those determined for the SiMeMes derivatives **2d**-DFT and **7d**-DFT, but there are notable differences that provide insight into how the SiMePh and SiMeMes groups influence the relative stabilities of these

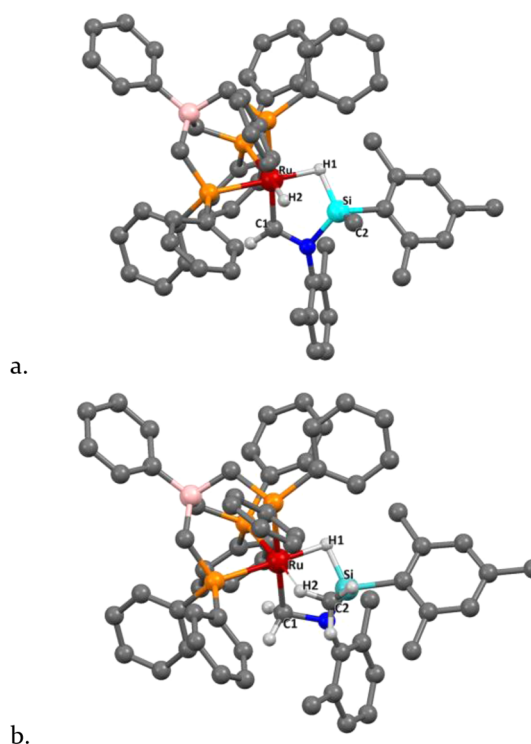


Figure 2. Structures determined by DFT calculations for the model compounds (a) **2d**-DFT and (b) **7d**-DFT. Note that a narrow bond line is used to denote the C–H→Ru interaction. In both structures, only selected hydrogen atoms are displayed in order to emphasize key interactions or functional group changes.

carbene and aminomethyl isomers. The model structure **2a**-DFT (Figure 3a) features two Ru–H–Si 3c 2e bonds in the form of an agostic Si–H→Ru 3c 2e bond ($d_{\text{Si-H1}} = 1.85$ Å, $d_{\text{Ru-H1}} = 1.66$ Å) and a Ru–H→Si interaction ($d_{\text{Si-H2}} = 2.18$ Å, $d_{\text{Ru-H2}} = 1.62$ Å). This latter type of interaction was not observed in the carbene structure **2d**-DFT, and this can be attributed to steric interactions between the [PhBP₃] ligand and the Si–Mes group that result in a longer Ru–Si distance for **2d**-DFT ($d_{\text{Ru-Si}} = 2.58$ Å) vs **2a**-DFT ($d_{\text{Ru-Si}} = 2.39$ Å). This results in a terminal Ru–H ligand in **2d**-DFT that is too far from silicon to engage in a significant Ru–H→Si interaction that would stabilize this hydride against 1,2-migration to the carbene ligand.^{7,19} Thus, the bulky Si–Mes group appears to destabilize the carbene structure **2d** by preventing the formation of a Ru–H→Si interaction like that which is observed to stabilize the SiMePh derivative **2a**.

Conversion of **2d** to **7d** moves the bulky Si–Mes group away from the [PhBP₃] ligand, while the much smaller SiCH₃ group is moved closer to ruthenium to engage in an agostic interaction ($d_{\text{Ru-HC}} = 2.09$ Å, **7d**-DFT, Figure 2). The SiCH₂–H→Ru interaction is promoted by the steric asymmetry of the SiMeMes group, and consequentially this agostic interaction is weaker in the SiMePh derivative **7a**-DFT ($d_{\text{Ru-HC}} = 2.81$ Å). This C–H agostic interaction replaces the hydride ligand that migrates from ruthenium to carbon to form the aminomethyl derivatives, and thereby helps stabilize the latter isomers. Thus, the bulk of the SiMeMes group promotes stability of the aminomethyl structure **7d** in addition to destabilizing the carbene isomer **2d**. These effects are less pronounced for the SiMePh derivatives, and the equilibrium for **2a/7a** more strongly favors the carbene structure **2a**.

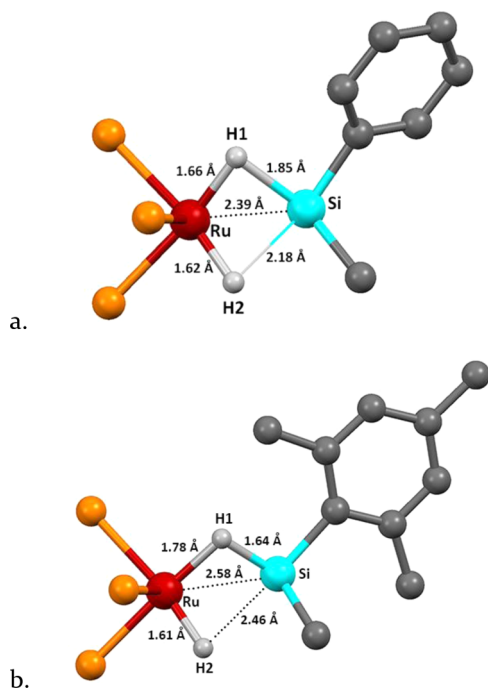
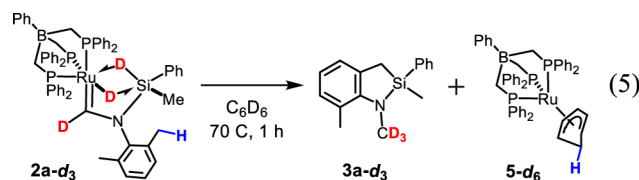


Figure 3. (a) View of the $P_3Ru(\mu-H)_2SiMePh$ portion of **2a**-DFT. (b) View of the $P_3Ru(H)(\mu-H)SiMeMes$ portion of **2d**-DFT. Note that all other atoms are omitted to facilitate easier comparison of the Ru–H and Si–H interactions. Thin lines denote relatively weak interactions, and dotted lines are drawn for nonbonded interatomic distances of interest.

If the aminomethyl complexes are intermediates in the formations of **3a** and **6**, then the equilibrium between the carbene (**2a,d**) and aminomethyl complexes (**7a,d**) might influence the relative rates at which the benzylic C–H activation products are formed. This possibility would explain the comparatively rapid conversion of **2d** to **6** (12 h at 23 °C) relative to the elimination of **3a** from **2a** (1 week at 23 °C). This hypothesis is further supported by examinations of the $SiPh_2$ (**2b**) and $SiEt_2$ (**2c**) carbene derivatives by 1H NMR spectroscopy in benzene- d_6 at 80 °C. At this temperature, these carbene complexes undergo conversion to the C–H activated products **3b,c**, which were not isolated but are readily identified *in situ* by the similarity of their 1H NMR spectra to that of **3a** (see [Supporting Information](#)). The relative rates for the formations of **3a–c** at 80 °C are (fastest to slowest): **3a** (ca. 90% conversion after 0.5 h at 80 °C) > **3c** (ca. 90% conversion after 4 h at 80 °C) > **3b** (ca. 80% after 20 h at 80 °C). These results indicate that the steric asymmetry of the $SiRR'$ group and the presence of a $Si-CH_2R$ group ($R = H$ or Me) increase the rate of conversion of **2a–c** to **3a–c**. Note that these are the same factors that appear to increase the stability of the aminomethyl complexes **7a–d** relative to their carbene isomers **2a–d**.

The formation of the silacycloindoline product **3a** was further examined by a deuterium labeling experiment using **2a-d₃**, prepared by treatment of $[PhBP_3]Ru(D)(\eta^3-D_2SiMePh)$ (**1a-d₃**) with XylNC (1 equiv). Complex **2a-d₃** (in benzene- d_6) undergoes conversion to **3a-d₃** with incorporation of all three deuteriums into an NCD_3 group (eq 5), as evident from the absence of the NCH_3 resonance in the 1H NMR spectrum after complete conversion of **2a-d₃** to **3a-d₃**. This result implies that formation of the NCD_3 group occurs prior to the C–H



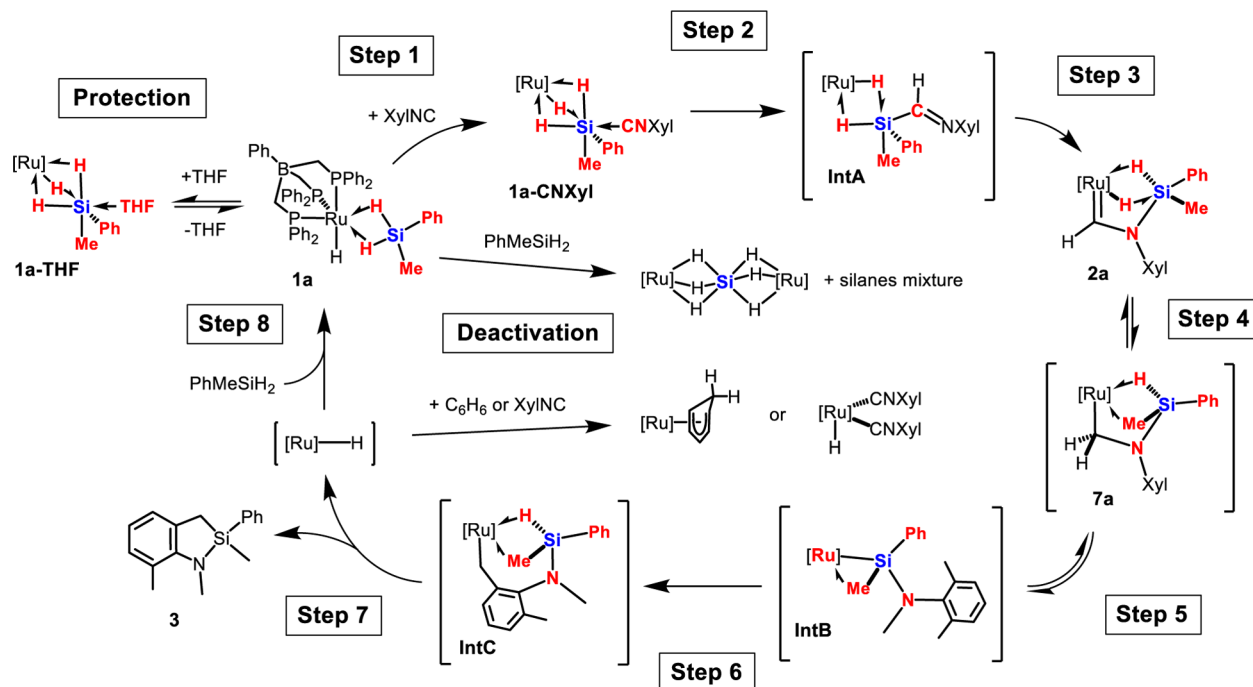
activation step, since the latter process would provide hydrogen that could be incorporated into the NMe group. Instead, the hydrogen originating from activation of the benzylic C–H bond appears to be incorporated into the cyclopentadienyl ligand of **5-d₆** (observed by 1H NMR spectroscopy). The complete incorporation of deuterium into the NCD_3 group implicates the elimination of this group from ruthenium to provide a 14-electron ruthenium silyl complex $[PhBP_3]Ru-Si(NMeXyl)MePh$ (IntB, [Scheme 5](#)) as the intermediate responsible for the benzylic C–H activation in the formation of **3**.

A remarkably large inverse kinetic isotope effect was observed for the conversion of **2a/2a-d₃** to **3a/3a-d₃** ($k_H/k_D = 0.48(2)$). This large inverse KIE might be due to an equilibrium isotope effect for formation of the NCH_3 group from the carbene ligand in **2a**. This process involves the formation of two C–H/D bonds, which is more favorable for deuterium than for hydrogen.²² Additionally, these C–H/D bonds are formed from hydrides in the bridging Ru–H–Si positions of **2a**, and this makes transfer of deuterium to the C–D positions particularly favorable relative to the proteo system.²² For these thermodynamic considerations to manifest as a large inverse KIE, the C–H/D bond-forming processes must be reversible, and these steps must precede the rate limiting step of the reaction. This implies that IntB can revert back to the carbene complex **2a**.

Interestingly, the conversion of IntB back to **2a** involves the double C–H activation of the NCH_3 group to form a carbene ligand with both resulting hydride ligands stabilized in the coordination sphere of ruthenium by Ru–H–Si 3c 2e interactions. In this regard, the $SiRR'$ fragment plays a similar role to that of tethered borane or boryl groups that assist transition metals in the activation of E–H bonds by the formation of M–H–B 3c 2e interactions.² Thus, the silicon center is critical for enabling the remarkable interconversion of the 14-electron silyl species and the 18-electron carbene species. Other metal complexes have been reported to activate NCH_3 groups to form Fischer carbene complexes, but those double C–H activations require complete removal of at least one hydride ligand from the metal center.²¹ As a result, these prior examples involve less dramatic changes of the electron count at the metal center than for interconversion of **3a** and IntB, and only this latter example engages in reversible interconversion of NCH_3 and $M=C(H)NR_2$ species.

Synthetic Cycle for the Formation of **3a.** [Scheme 5](#) depicts a cycle for the formation of **3a** (in THF) that is consistent with experimental and theoretical investigations of reactions of XylNC with **1a–d**. A variety of different classical and nonclassical silicon species appear in this mechanism (note that the coordination environments of silicon are highlighted in red in [Scheme 5](#)), which starts with the off-cycle species **1a**-THF that features THF bound to a hexacoordinate silicon center. This adduct is not an intermediate in the formation of **3a**, but as described above, the binding of THF to silicon plays an important role in successful pseudocatalytic turnover because the unbound $\eta^3-H_2SiMePh$ complex **1a** catalyzes

Scheme 5. Experimentally Determined Synthetic Cycle for the Formation of C–H Functionalized Product 3a



detrimental silane redistribution reactions under conditions necessary to fully regenerate **1a** from **2a**. These redistribution reactions result in formation of the unreactive diruthenium hexahydrosilicate complex $\{[\text{PhBP}_3]\text{Ru}\}_2[\eta^4, \eta^4\text{-H}_6\text{Si}]$,^{12b} which is not reactive. The coordination of THF to silicon in **1a-THF** appears to inhibit these undesired Si–C bond cleavage processes, and this protects the catalyst from deactivation while all of **2a** undergoes conversion to **3a** and **1a-THF**.

The THF adduct (**1a-THF**) has previously been demonstrated to dissociate readily to form **1a**,^{12a} which is an intermediate in the productive cycle. As described above, the isocyanide binds to the silicon center of **1a** to form a hexacoordinate silicon adduct **1a-CNXYl**. The isocyanide then undergoes insertion into the Si–H portion of a Ru–H–Si 3c 2e bond, and the resulting intermediate **IntA** rapidly isomerizes to the carbene species **2a**. This latter step is reminiscent of the unique property of acylsilanes ($\text{R}_3\text{SiC(R')=O}$) to isomerize to transient carbene species even in the absence of transition metals.²³ The rearrangement of the Si–C(H)=NXYl group to the carbene complex **2a** is important since this isomerization activates the carbon atom to accept both hydrides from the Ru–H–Si positions. This allows the carbene complex **2a** to undergo a double C–H elimination and exist in equilibrium with a four coordinate 14-electron ruthenium silyl intermediate (**IntB**, Scheme 5). The interconversion of **2a** and **IntB** involves competing influences of the SiMePh fragment: Ru–H–Si interactions stabilize the hydride ligands in **2a**, whereas the SiMe group offers agostic $\text{SiCH}_2\text{-H}\rightarrow\text{Ru}$ interactions in **7a** and **IntB** that help stabilize the coordinatively unsaturated ruthenium center resulting from elimination of the hydrides.

The 14-electron ruthenium silyl complex **IntB** is expected to be highly reactive and is implicated in the key benzylic C–H bond activation step to form **IntC** (Scheme 5). Note that **IntC** is similar in structure to isolated complex **6**, except that **6** features a benzyl ligand derived from a Si–Me group rather than an N–Xyl group. In both these species, the hydride ligand derived from the benzylic C–H bond is stabilized by the

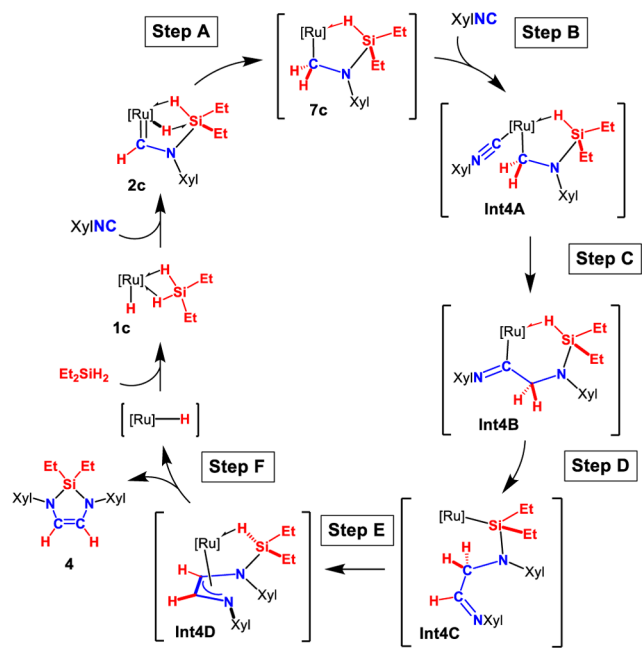
formation of an Si–H \rightarrow Ru moiety, thus demonstrating a similarity with C–H activations that are supported by M–H–B 3c 2e bond formation.²

The exact nature of the C–Si bond-forming step is unclear, but it seems reasonable that the Si–H group in **IntC** might engage in a σ -bond metathesis process with the Ru–C bond to form the Si–C bond of the final product **3a**. The elimination of **3a** generates a highly reactive Ru–H intermediate, tentatively described as the 14-electron species $[\text{PhBP}_3]\text{RuH}$. This hydride intermediate was not directly observed, and may exist with stabilization from coordinated solvent. This hydride species has previously been trapped with benzene to form the cyclohexadienyl complex **5**,¹⁴ which prevents turnover of catalysis with benzene as solvent. The hydride intermediate is presumably more robust in the absence of benzene, and this is evident from the regeneration of the $\eta^3\text{-H}_2\text{SiMePh}$ complex **1a** with THF- d_8 as the solvent, but not with benzene- d_6 . Complex **1a** is rapidly trapped and protected as the THF adduct **1a-THF** that is observed (by ^1H NMR spectroscopy) after full conversion of **2a** to the organosilicon product **3a**.

Overall, the mechanism and intermediates depicted in Scheme 5 are well supported by experimental observations. Many of the proposed intermediates were isolated (e.g., **1a** and **2a**) or directly observed (e.g., **1a-THF** and **1a-CNXYl**). Other intermediates have been studied as model compounds that were isolated or observed (e.g., **7d** is a model for **7a**, and **6** serves as a model for **IntC**). The remaining proposed ruthenium–silicon intermediates (e.g., **IntA** and **IntB**) were implicated by experimental observations and computational studies.

Catalytic Cycle for the Formation of 4. The formation of the C=C reductive coupling product **4** also appears to depend on multiple nonclassical ruthenium–silicon intermediates (Scheme 6) that interconvert via processes related to those demonstrated in the formation of **3a** (Scheme 5). As described above, the initial isocyanide activation by **1c** occurs via the same pathway involving 5- and 6-coordinate silicon intermediates as

Scheme 6. Possible Mechanism to Produce 4



is involved in the formation of the carbene complex **2a** (Scheme 5, steps 1 and 2). After activation of the first equivalent of isocyanide, equilibration between **2c** and a 16-electron aminomethyl complex **7c** (Scheme 6, step A) provides a pathway by which the second equivalent of isocyanide can be introduced to ruthenium (step B). The resulting intermediate (Int4A) might facilitate C–C bond formation by migratory insertion of the isocyanide into the Ru–C bond of the aminomethyl group (step C) to form Int4B. Formation of the aminoacyl C–H bond (step D) would produce the 14-electron ruthenium silyl complex (Int4C) that is similar to IntB implicated in the formation of **3a**. These low coordinate silyl complexes are highly reactive, and Int4C likely undergoes rapid activation of a SiNC–H bond to form Int4D (step E), which is a process analogous to activation of the NCH₃ group by IntB (i.e., the reverse of step 5 in Scheme 5). Finally, elimination of a Si–N bond from Int4D (step F) would provide the product **4** and generate a ruthenium hydride complex that binds Et₂SiH₂ to reform the η³-H₂SiEt₂ complex **1c**.

The mechanism proposed for the formation of **4** could not be verified to the extent that the mechanism for the formation of **3a** was established, since intermediates in the formation of **4** from **2c** and XylNC could not be identified. However, the proposed intermediates and reaction steps of Scheme 6 are supported by well-established chemistry (e.g., migratory insertion involving isocyanides)²⁴ and by experimental observation of similar intermediates and reaction steps identified in the formation of **3a**. Other mechanisms might be possible for the formation of **4**; for example, the mechanism might involve attack of isocyanide onto the carbene carbon of **2c** to facilitate C–C bond formation.²⁵ Regardless of the exact mechanism of the C–C bond forming step, the formation of **4** clearly involves multiple Ru–H–Si species, and thus demonstrates the ability of these unusual structures to mediate this notable C=C bond forming process.

CONCLUSION

Two novel transformations for secondary silanes (e.g., RR'SiH₂, RR' = MePh, Et₂) and XylNC were discovered, and these transformations are enabled by a unique isocyanide activation process involving the electrophilic η³-H₂SiRR' complexes **1a–d**. In one reaction, Et₂SiH₂ serves as the reducing agent in the reductive coupling of two isocyanides to form a C=C bond. Catalytic turnover in the synthesis of **4** was observed, though turnover in the current system is limited by deactivation of the catalyst. To our knowledge, homogeneous catalysts have not previously been capable of mediating this type of C₁–C₁ coupling reaction. Furthermore, the formation of **4** is notable since the silane is a mild reducing agent relative to the strong reducing agents (e.g., Zn⁰, Na⁰, Cr(I), Mg(I), U(III)) often utilized for stoichiometric reductive couplings of isocyanides¹¹ or the closely related substrate CO.¹⁰

A different transformation is observed with XylNC and PhMeSiH₂, to form the C–H functionalized product **3a**. Interestingly, this process appears to involve sequential hydrosilylation and hydrogenation of the isocyanide group, which is then followed by conversion of a C–H bond to a C–Si bond. Though the formation of **3a** is not a practical catalytic process, it is interesting as a novel advance toward development of atom-economical C–H functionalizations. In particular, a single functional group (–N≡C) plays multiple roles in this transformation, and this group is incorporated into the final product as a common functionality (NCH₃). This type of C–H functionalization could conceivably be adapted to other substrates that might undergo both a hydrosilylation and a hydrogenation process (for example, alkynyl groups).

A fascinating aspect of the formation of **3a** and **4** is the unusual mechanisms by which these products form. The mechanism for the formation of **3a**, examined in particular detail, involves a remarkable variety of distinct coordination environments exhibited by silicon: two hexacoordinate silicon species (**1a**-THF and **1a**-CNXyl), two pentacoordinate silicon species (IntA and **2a**), and four tetracoordinate silicon intermediates (**1a**, **7a**, IntB, and IntC). In total, seven different silicon coordination environments are involved in this transformation, and many of these involve one or more M–H–Si 3c 2e bonds. A variety of unusual M–(H)_n–Si (*n* = 2–3) structures have been discovered in the past two decades,⁷ but the role of these species in catalysis has previously been limited primarily to examples of simple Si–O or Si–C bond-forming reactions.²⁶ Thus, it is quite notable that several unusual silicon structures are involved in an intricate cycle that culminates in a C–H functionalization.

The unusual hypercoordinate silicon-based ligands play a variety of roles to assist ruthenium in transforming the isocyanide substrate to form **3a** and **4**. It is notable that these cooperative effects are observed using a stoichiometric silane reagent since there are an increasing number of reduction reactions and catalytic C–H functionalization reactions involving silane reactants or silyl directing groups.^{16,27} It is conceivable that the silicon center also plays a complex role in some examples of these reactions. The role of silicon in forming **3a** and **4** might also inform efforts to design cooperative ligands that utilize silicon in catalytic transformations. This possibility is bolstered by the participation of silicon in parts of the isocyanide transformations that do not directly form bonds to silicon (e.g., hydrogenation of the isocyanide, benzylic C–H activation, NCH₃ double C–H activation, C=C bond

formation). These processes illustrate a variety of ways that silicon can cooperate with a transition metal without the silicon species necessarily being consumed.

■ ASSOCIATED CONTENT

Supporting Information

The Supporting Information is available free of charge on the ACS Publications website at DOI: 10.1021/jacs.6b05736.

Crystal data for compound **6** (CIF)

Synthetic details and characterization data for new compounds (**2c**, **2e**, **3a**, **4**, and **6**), in situ NMR data (for **2d** and **7d**), computational details, and details of kinetics measurements and deuterium labeling experiments (PDF)

■ AUTHOR INFORMATION

Corresponding Author

*tdtilley@berkeley.edu

Present Addresses

[†]M.C.L.: Department of Chemistry, Northwestern University, 2145 Sheridan Rd, Evanston, IL 60208.

[‡]A.L.L.-M.: Division of Chemistry and Chemical Engineering, California Institute of Technology, 1200 East California Blvd, Pasadena, CA 91125.

Notes

The authors declare no competing financial interest.

■ ACKNOWLEDGMENTS

This work was funded by the National Science Foundation under Grant No. CHE-1566538. The molecular graphics and computational facility (College of Chemistry, University of California, Berkeley) is supported by the National Science Foundation under Grant No. CHE-0840505.

■ REFERENCES

(1) For the purpose of this discussion, “cooperation between transition metals and semimetals” includes reactivity in which the semimetal is incorporated into the product, but actively participates with the transition metal center in the transformation. Examples: B–H and Si–H bond formations that assist C–H activations (see refs **2b**, **c** and **3a**, **b**); B–O bond formations that assist C–C reductive coupling (see refs **9a**, **b**).

(2) (a) Devillard, M.; Bouhadir, G.; Bourissou, D. *Angew. Chem., Int. Ed.* **2015**, *54*, 730–732. (b) Webster, C. E.; Fan, Y.; Hall, M. B.; Kunz, D.; Hartwig, J. F. *J. Am. Chem. Soc.* **2003**, *125*, 858–859. (c) Tamura, H.; Yamazaki, H.; Sato, H.; Sakaki, S. *J. Am. Chem. Soc.* **2003**, *125*, 16114–16126. (d) Harman, W. H.; Peters, J. C. *J. Am. Chem. Soc.* **2012**, *134*, 5080–5082. (e) MacMillan, S. N.; Harman, W. H.; Peters, J. C. *Chem. Sci.* **2014**, *5*, 590–597. (f) Lin, T.-P.; Peters, J. C. *J. Am. Chem. Soc.* **2013**, *135*, 15310–15313. (g) Suess, D. L. M.; Peters, J. C. *J. Am. Chem. Soc.* **2013**, *135*, 12580–12583. (h) Barnett, B. R.; Moore, C. E.; Rheingold, A. L.; Figueroa, J. S. *J. Am. Chem. Soc.* **2014**, *136*, 10262–10265. (i) Cowie, B. E.; Emslie, D. J. H. *Chem. - Eur. J.* **2014**, *20*, 16899. (j) Cassen, A.; Gloaguen, Y.; Vendier, L.; Duhayon, C.; Poblador-Bahamonde, A.; Raynaud, C.; Clot, E.; Alcaraz, G.; Sabo-Etienne, A. *Angew. Chem., Int. Ed.* **2014**, *53*, 7569–7573.

(3) (a) Sadow, A. D.; Tilley, T. D. *J. Am. Chem. Soc.* **2002**, *124*, 6814–6815. (b) Sadow, A. D.; Tilley, T. D. *J. Am. Chem. Soc.* **2005**, *127*, 643–656. (c) Ochiai, M.; Hashimoto, H.; Tobita, H. *Angew. Chem., Int. Ed.* **2007**, *46*, 8192–8194. (d) Komuro, T.; Arai, T.; Kikuchi, K.; Tobita, H. *Organometallics* **2015**, *34*, 1211–1217. (e) Lee, C.-I.; Zhou, J.; Ozerov, O. V. *J. Am. Chem. Soc.* **2013**, *135*, 3560–3566. (f) Lee, C.-I.; Hirscher, N. A.; Zhou, J.; Bhuvanesh, N.; Ozerov, O. V. *Organometallics* **2015**, *34*, 3099–3102. (g) Montiel-Palma, V.; Muñoz-

Hernández, M. A.; Ayed, T.; Barthelat, J.-C.; Grellier, M.; Vendier, L.; Sabo-Etienne, S. *Chem. Commun.* **2007**, 3963–3965. (h) Dioumaev, V. K.; Carroll, P. J.; Berry, D. H. *Angew. Chem., Int. Ed.* **2003**, *42*, 3947–3949.

(4) Hashimoto, H.; Fukuda, T.; Tobita, H.; Ray, M.; Sakaki, S. *Angew. Chem., Int. Ed.* **2012**, *51*, 2930–2933.

(5) (a) Waterman, R.; Hayes, P. G.; Tilley, T. D. *Acc. Chem. Res.* **2007**, *40*, 712–719. (b) Okazaki, M.; Tobita, H.; Ogino, H. *Dalton Trans.* **2003**, 493–506. (c) Hayes, P. G.; Xu, Z.; Beddie, C.; Keith, J. M.; Hall, M. B.; Tilley, T. D. *J. Am. Chem. Soc.* **2013**, *135*, 11780–11783. (d) Filippou, A. C.; Chernov, O.; Stumpf, K. W.; Schnakenburg, G. *Angew. Chem., Int. Ed.* **2010**, *49*, 3296–330.

(6) (a) Hillier, A. C.; Jacobsen, H.; Gusev, D.; Schmalte, H. W.; Berke, H. *Inorg. Chem.* **2001**, *40*, 6334–6337. (b) Alcaraz, G.; Clot, E.; Helmstedt, U.; Vendier, L.; Sabo-Etienne, S. *J. Am. Chem. Soc.* **2007**, *129*, 8704–8705. (c) Alcaraz, G.; Helmstedt, U.; Clot, E.; Vendier, L.; Sabo-Etienne, S. *J. Am. Chem. Soc.* **2008**, *130*, 12878–12879. (d) Maekawa, M.; Daniliuc, C. G.; Jones, P. G.; Hohenberger, J.; Sutter, J.; Meyer, K.; Walter, M. D. *Eur. J. Inorg. Chem.* **2013**, *2013*, 4097–4104. (e) Braunschweig, H.; Gackstatter, A.; Kupfer, T.; Radacki, K.; Franke, S.; Meyer, K.; Fucke, K.; Lemée-Cailleau, M.-H. *Inorg. Chem.* **2015**, *54*, 8022–8028.

(7) (a) Nikonov, G. I. *Angew. Chem., Int. Ed.* **2001**, *40*, 3353–3355. (b) Lachaize, S.; Sabo-Etienne, S. *Eur. J. Inorg. Chem.* **2006**, *2006*, 2115–2127. (c) Corey, J. Y. *Chem. Rev.* **2011**, *111*, 863–107.

(8) (a) Ueno, K.; Yamaguchi, K.; Ogino, H. *Organometallics* **1999**, *18*, 4468–4470. (b) Filippou, A. C.; Weidemann, N.; Philippopoulos, A. I.; Schnakenburg, G. *Angew. Chem., Int. Ed.* **2006**, *45*, 5987–5991. (c) Hayes, P. G.; Waterman, R.; Glaser, P. B.; Tilley, T. D. *Organometallics* **2009**, *28*, 5082–5089. (d) Filippou, A. C.; Barandov, A.; Schnakenburg, G.; Lewall, B.; van Gastel, M.; Marchanka, A. *Angew. Chem., Int. Ed.* **2012**, *51*, 789–793. (e) Fasulo, M.; Tilley, T. D. *Chem. Commun.* **2012**, *48*, 7690–7692. (f) Inomata, K.; Watanabe, T.; Tobita, H. *J. Am. Chem. Soc.* **2014**, *136*, 14341–14344.

(9) (a) Miller, A. J. M.; Labinger, J. A.; Bercaw, J. E. *J. Am. Chem. Soc.* **2008**, *130*, 11874–11875. (b) Miller, A. J. M.; Labinger, J. A.; Bercaw, J. E. *J. Am. Chem. Soc.* **2010**, *132*, 3301–3303.

(10) (a) Wolczanski, P.; Bercaw, J. E. *Acc. Chem. Res.* **1980**, *13*, 121–127. (b) Herrmann, W. A. *Angew. Chem., Int. Ed. Engl.* **1982**, *21*, 117–130. (c) Khodakov, A. Y.; Chu, W.; Fongarland, P. *Chem. Rev.* **2007**, *107*, 1692–1744. (d) West, N. M.; Miller, A. J. M.; Labinger, J. A.; Bercaw, J. E. *Coord. Chem. Rev.* **2011**, *255*, 881–898. (e) Bianconi, P. A.; Williams, I. D.; Engeler, M. P.; Lippard, S. J. *J. Am. Chem. Soc.* **1986**, *108*, 311–313. (f) Gardner, B. M.; Stewart, J. C.; Davis, A. L.; McMaster, J.; Lewis, W.; Blake, A. J.; Liddle, S. T. *Proc. Natl. Acad. Sci. U. S. A.* **2012**, *109*, 9265–9270. (g) Summerscales, O. T.; Cloke, F. G. N.; Hitchcock, P. B.; Green, J. C.; Hazari, N. *Science* **2006**, *311*, 829–831. (h) Braunschweig, H.; Dellermann, T.; Dewhurst, R. D.; Ewing, W. C.; Hammond, K.; Jimenez-Halla, J. O. C.; Kramer, T.; Krummenacher, I.; Mies, J.; Phukan, A. K.; Vargas, A. *Nat. Chem.* **2013**, *5*, 1025–1028.

(11) (a) Carnahan, E. M.; Protasiewicz, J. D.; Lippard, S. J. *Acc. Chem. Res.* **1993**, *26*, 90–97. (b) Boyarskiy, V. P.; Bokach, N. A.; Luzyanin, K. V.; Kukushkin, V. Y. *Chem. Rev.* **2015**, *115*, 2698–2779. (c) Lam, C. T.; Corfield, P. W. R.; Lippard, S. J. *J. Am. Chem. Soc.* **1977**, *99*, 617–618. (d) Shen, J.; Yap, G. P. A.; Theopold, K. H. *J. Am. Chem. Soc.* **2014**, *136*, 3382–3384.

(12) (a) Lipke, M. C.; Tilley, T. D. *J. Am. Chem. Soc.* **2011**, *133*, 16374–16377. (b) Lipke, M. C.; Tilley, T. D. *Angew. Chem., Int. Ed.* **2012**, *51*, 11115–11121.

(13) Lipke, M. C.; Tilley, T. D. *J. Am. Chem. Soc.* **2013**, *135*, 10298–10301.

(14) Lipke, M. C.; Neumeyer, F.; Tilley, T. D. *J. Am. Chem. Soc.* **2014**, *136*, 6092–6102.

(15) Liepins, E.; Birgele, I.; Tomsons, P.; Lukevics, E. *Magn. Reson. Chem.* **1985**, *23*, 485–486.

(16) Cheng, C.; Hartwig, J. F. *Chem. Rev.* **2015**, *115*, 8946–8975.

(17) Cui, H.; Shao, Y.; Li, X.; Kong, L.; Cui, C. *Organometallics* **2009**, *28*, 5191–5195.

(18) Several structures containing [PhBP₃]Ru, SiRR', and SiRR'L moieties have previously been reported (see ref 12). Thus, the bond lengths and angles determined by XRD for compound **6** could be compared to highly analogous structures. This analysis indicates no significant deviation of these quantitative parameters for the structure of **6** from expectations based on related higher quality structures. Additionally, the connectivity illustrated in the structure of **6** is verified in solution by a variety of NMR techniques. Thus, we conclude that the determined structure is a valid depiction of the connectivity of **6**, but caution that this conclusion cannot be reached solely based on the diffraction data for **6**. See page S27 in the [Supporting Information](#) for further information about the limitations of the diffraction data.

(19) (a) Schubert, U. *Adv. Organomet. Chem.* **1990**, *30*, 151–187. (b) Yang, J.; White, P. S.; Schauer, C. K.; Brookhart, M. *Angew. Chem., Int. Ed.* **2008**, *47*, 4141–4143.

(20) Calculations were performed using the B3PW91 hybrid functional with the 6-31G(d,p) basis set for all main-group elements and the LANL 2DZ basis set for ruthenium.

(21) Rankin, M. A.; McDonald, R.; Ferguson, M. J.; Stradiotto, M. *Angew. Chem., Int. Ed.* **2005**, *44*, 3603–3606.

(22) (a) Calvert, R. B.; Shapley, J. R. *J. Am. Chem. Soc.* **1978**, *100*, 7726–7727. (b) Brookhart, M.; Green, M. L. H. *J. Organomet. Chem.* **1983**, *250*, 395–408.

(23) (a) Bassindale, A. R.; Brook, A. G.; Harris, J. J. *Organomet. Chem.* **1975**, *90*, C6–C8. (b) Brook, A. G. *Acc. Chem. Res.* **1974**, *7*, 77–84.

(24) (a) Lee, J. P.; Pittard, K. A.; DeYonker, N. J.; Cundari, T. R.; Gunnoe, T. B.; Petersen, J. L. *Organometallics* **2006**, *25*, 1500–1510. (b) Kofod, P.; Harris, P.; Larsen, S. *Inorg. Chem.* **2003**, *42*, 244–249. (c) Zhu, C.; Xie, W.; Falck, J. R. *Chem. - Eur. J.* **2011**, *17*, 12591–12595. (d) Vicente, J.; Chicote, M. T.; Vicente-Hernández, I.; Bautista, D. *Inorg. Chem.* **2007**, *46*, 8939–8949.

(25) (a) Campion, B. K.; Heyn, R. H.; Tilley, T. D. *J. Am. Chem. Soc.* **1990**, *112*, 2011–2013. (b) Radu, N. S.; Engeler, M. P.; Gerlach, C. P.; Tilley, T. D.; Rheingold, A. L. *J. Am. Chem. Soc.* **1995**, *117*, 3621–3622.

(26) (a) Lipke, M. C.; Tilley, T. D. *J. Am. Chem. Soc.* **2014**, *136*, 16387–16398. (b) Gutsulyak, D. V.; Kuzmina, L. G.; Howard, J. A. K.; Vyboishchikov, S. F.; Nikonov, G. I. *J. Am. Chem. Soc.* **2008**, *130*, 3732–3733. (c) Lee, T. Y.; Dang, L.; Zhou, Z.; Yeung, C. H.; Lin, Z.; Lau, C. P. *Eur. J. Inorg. Chem.* **2010**, *36*, 5675–5684. (d) Lachaize, S.; Vendier, L.; Sabo-Etienne, S. *Dalton Trans.* **2010**, *39*, 8492–8500. (e) Fasulo, M.; Lipke, M. C.; Tilley, T. D. *Chem. Sci.* **2013**, *4*, 3882–3887.

(27) (a) Yang, J.; Brookhart, M. *J. Am. Chem. Soc.* **2007**, *129*, 12656–12657. (b) Cheng, C.; Brookhart, M. *J. Am. Chem. Soc.* **2012**, *134*, 11304–11307. (c) Cheng, C.; Brookhart, M. *Angew. Chem., Int. Ed.* **2012**, *51*, 9422–9424. (d) Xu, S.; Boschen, J. S.; Biswas, A.; Kobayashi, T.; Pruski, M.; Windus, T. L.; Sadow, A. D. *Dalton Trans.* **2015**, *44*, 15897–15904. (e) Jacquet, O.; Frogneux, X.; Gomes, C. D. N.; Cantat, T. *Chem. Sci.* **2013**, *4*, 2127–2131.